Molecular Mechanism of GTP Hydrolysis by Bovine Transducin: Pre-Steady-State Kinetic Analyses†

Tuow Daniel Ting and Yee-Kin Ho*

Departments of Biochemistry and Ophthalmology, University of Illinois at Chicago, Health Sciences Center, 1853 West Polk Street, Chicago, Illinois 60612

Received December 26, 1990; Revised Manuscript Received June 28, 1991

ABSTRACT: During the visual transduction process in rod photoreceptor cells, transducin (T) mediates the flow of information from photoexcited rhodopsin (R*) to the cGMP phosphodiesterase (PDE) via a cycle of GTP binding and hydrolysis. The pre-steady-state kinetics of GTP hydrolysis by T was studied by rapid quenching and filtration techniques in a reconstituted system containing purified R* and T. Kinetic analyses have shown that the turnover of T-bound GTP can be dissected into four partial reactions: (1) the R*-catalyzed GTP binding via a GDP/GTP exchange reaction, (2) the on-site hydrolysis of bound GTP, which leads to the formation of a T–GDP·P_i complex, (3) the release of the tightly bound inorganic phosphate (P_i) from T–GDP·P_i, and (4) the recycling of T–GDP. The R*-catalyzed GTP binding was estimated to occur in <1 s. In rapid acid quenching experiments, the rate of P_i formation due to GTP hydrolysis exhibited biphasic characteristics. An initial burst of P_i formation occurred between 1 and 4 s, which was followed by a slow steady-state rate. Increasing T concentration yielded a proportional increase in the burst and steady-state rate. The addition of Gpp(NH)p decreased both parameters. D_2O decreased the rise of the initial burst with a kinetic isotope effect of ~1.7 but has no effect on the steady-state rate of P_i formation. These results indicate that the burst represents the fast hydrolysis of GTP at the binding site of T, which results in the accumulation of T–GDP·P_i complexes. The steady-state rate represents the slow release of P_i. This finding was further supported by rapid filtration experiments that monitored the formation of free P_i in solution. An initial lag time in the formation of free P_i was observed before a steady-state rate was established, indicating that the initially formed P_i was tightly bound to T. Finally, the release of GDP from T–GDP·P_i was not detected. This suggests that another cycle of GTP exchange catalyzed by R* should occur before the release of bound GDP. The rate of P_i release from T–GDP·P_i was measured under single-turnover conditions and had a half life of ~20 s, which was identical with the rate of deactivation of the PDE due to GTP hydrolysis by T. This suggests that T–GDP·P_i possesses a conformation similar to that of T–GTP, and is capable of activating the latent PDE, and the release of tightly bound P_i from T–GDP·P_i is the rate-limiting step in turning off activated T. The addition of purified PDE or 48K protein (arrestin) had no effect on the pre-steady-state kinetics of GTP hydrolysis. This indicates that the interaction between T and PDE does not alter the turnover rate of GTP hydrolysis by T. On the basis of the kinetics, the T–GDP·P_i complex represents the major species that activates PDE. Since the deactivation of transducin by the release of tightly bound P_i takes >20 s, one may assume that GTP hydrolysis by transducin cannot be the turn off mechanism for the cGMP cascade, which occurs within a few seconds under physiological condition [Sitaramayya, A., & Liebman, P. A. (1983) *J. Biol. Chem. 258*, 12106–12109].

Visual excitation involves the conversion of a stimulus in the form of light to neural signals. In vertebrate rod photoreceptor cells, this process involves the activation of a cGMP enzyme cascade in the rod outer segment (ROS).[1] The ROS disk membrane contains membrane-bound proteins of the cGMP cascade, such as rhodopsin (R), transducin (T), and cGMP phosphodiesterase (PDE). The ROS plasma membrane contains channels whose permeability to Na^+ ions is controlled by the level of intracellular cGMP. In dark-adapted rod cells, the cGMP cascade is inactive, and the cytosolic concentration of cGMP is relatively high (~60 μM) (Woodruff & Fain, 1982). This maintains a large fraction of the cGMP-sensitive channels in the open state (Fesenko et al., 1985) and keeps the cell relatively depolarized. Photoexcited rhodopsin (R*) binds transducin and catalyzes a GDP/GTP exchange reaction that converts transducin to an active form of T–GTP. T–GTP then activates PDE by relieving the restraint exerted by the P_γ inhibitory subunit of PDE (Fung & Stryer, 1980; Fung et al., 1981; Hurley & Stryer, 1982). A single R* can generate hundreds of T–GTP, and each T–GTP is capable of activating PDE. This leads to the rapid hydrolysis of thousands of molecules of cGMP per second. As the level of cGMP in ROS is reduced, the cGMP–sensitive channels start to close and the cell hyperpolarizes. The photoexcitation signal is thus transduced to a neural signal recognizable by other cells in the retina [for reviews, see Liebman et al. (1987), Stryer (1986), and Applebury and Hargrave (1986)].

† We dedicate this paper to Professor Jui H. Wang on the occasion of his 70th birthday. This work was supported by Grant EY-05788 from the National Eye Institute and in part by a BRSG Award from the Biomedical Research Support Grant Program of the NIH. Part of this work was presented at the 1989 ARVO annual meeting (Sarasota, FL).

* To whom correspondence should be addressed.

[1] Abbreviations: T, transducin; T_α and $T_{\beta\gamma}$, the α and βγ subunits of transducin; PDE, cyclic GMP phosphodiesterase; P_γ, the inhibitory subunit of PDE; $P_{\alpha\beta}$, the catalytic subunits of PDE; R*, photoexcited rhodopsin; SDS, sodium dodecyl sulfate; Gpp(NH)p, guanosine 5′-(β,γ-imidotriphosphate); DTT, dithiothreitol; MOPS, 4-morpholinepropanesulfonic acid; Tris, tris(hydroxymethyl)aminomethane; D_2O, deuterium oxide, heavy water; P_i, inorganic phosphate; FITC, fluorescein 5′-isothiocyanate; EDTA, ethylenediaminetetraacetic acid; ROS, rod outer segment; DEAE, diethylaminoethyl; E_a, activation energy.

0006-2960/91/0430-8996$02.50/0

In order for the rod cell to be repeatedly responsive to continuous cycles of stimulation by light, the cascade has to be turned off rapidly and the cGMP level restored to the dark-adapted level. The inhibitory regulation of the cascade at the rhodopsin level is mediated by the phosphorylation of R* by rhodopsin kinase, which converts R* to a form that binds the 48-kDa cytosolic protein, arrestin (Liebman & Pugh, 1980; Wilden et al., 1986a; Sitaramayya & Liebman, 1983). The binding of this 48-kDa protein to phosphorylated R* blocks further activation of transducin (Wilden et al., 1986a). Deactivation of the cascade at the transducin level is achieved when bound GTP is hydrolyzed to GDP (Fung et al., 1981). Once T–GTP is removed, the inhibitory P_γ subunit will recombine with the catalytic $P_{\alpha\beta}$ subunits to form an inhibited PDE (Hurley & Stryer, 1982). The goal of this study is to investigate the reaction dynamics of transducin during its coupling of the cGMP cascade; more specifically, to determine the kinetics of the GTP-binding and hydrolysis reactions that dictate the coupling function of transducin. The information obtained provides new insights on the coupling mechanism of transducin and the overall regulation of the cGMP cascade.

Experimental Procedures

Materials. Dark-adapted bovine eyes were obtained fresh from Brown Packing Co., South Holland, Illinois. The retinas were dissected in the dark and stored at −70 °C. Hexylagarose and ω-aminooctylagarose were products of Miles Laboratories. GTP and Gpp(NH)p were from P-L Biochemicals. Radioactive [^{32}P]GTP (15 Ci/mmol) and [^{3}H]GTP (10 Ci/mmol) were obtained from ICN Radiochemicals. Deuterium oxide (D_2O, 99.8 atom % D), DCl (18 wt % solution in D_2O, 100 atom % D), and NaOD (30 wt % solution in D_2O, 99+ atom % D) were from Aldrich. All other reagents were of the highest purity available. Buffer A (ROS stripping buffer, pH 7.5) contained 2 mM MOPS, 1 mM DTT, and 1 mM EDTA. Buffer B (GTPase assay buffer, pH 7.5) contained 10 mM MOPS, 200 mM NaCl, 2 mM $MgCl_2$, and 2 mM DTT. Buffer C (single-turnover dilution buffer, pH 7.5) contained 100 mM KH_2PO_4 and 2 mM $MgCl_2$. Buffer D (PDE assay buffer, pH 7.5) contained 10 mM MOPS, 200 mM NaCl, and 2 mM $MgCl_2$.

Isolation of ROS Membranes and Proteins. ROS disk membranes were isolated from bovine retinas by the sucrose flotation method, and rhodopsin in reconstituted membranes was prepared by the detergent dialysis method (Hong & Hubbell, 1973). Stripped ROS membranes void of transducin and PDE activities were prepared by washing the isolated ROS membranes six times with buffer A. The rhodopsin content was determined from the absorbance at 498 nm with a molar extinction coefficient of 42 700 cm^{-1} M^{-1}. Photolyzed ROS membranes were obtained by illuminating the dark-adapted membrane on ice under a fluorescent lamp for 15 min. The R* exist mostly in the meta II photo-intermediate state, which is stable at 0 °C for more than 6 h. Transducin was extracted from photolyzed ROS membrane with GTP and purified by hexylagarose column chromatography according to Fung (1983). T_α and $T_{\beta\gamma}$ were separated from purified transducin by ω-aminooctylagarose column chromatography (Ho & Fung, 1984). The latent PDE was obtained from low ionic strength extract of ROS membranes and subsequently purified by DEAE-Sephadex, ω-aminooctylagarose, and G-200 gel filtration chromatographies (Hurley & Stryer, 1982). SDS–polyacrylamide gel electrophoresis with subsequent Coomassie blue staining revealed that the purified T_α sample contained a single polypeptide of 40 kDa and no residual $T_{\beta\gamma}$. Purified $T_{\beta\gamma}$ showed two major bands at 36 and 8 kDa with ~2% contamination of T_α. Arrestin was purified according to the method by Wilden et al. (1986b) and appeared as a single band of 48-kDa protein with no contamination of transducin. Purified PDE contained three bands of 88, 84, and 14 kDa. All purified proteins were stored in buffer B with 40% glycerol at −20 °C.

Preparation of Samples in D_2O Buffer. All buffer solutions including those containing nucleotides were first prepared in H_2O with the pH of the solutions adjusted to the appropriate values with a Radiometer PHM 82 pH meter. The solution was then divided into two equal parts and lyophilized to dryness. These two fractions were then redissolved in a small amount of either H_2O or D_2O. In the D_2O sample, all the exchangeable hydrogen on the buffer molecules or nucleotides are replaced by deuterium. The solutions were again lyophilized to dryness and subsequently dissolved in H_2O or D_2O according to the original volume, which gave the correct buffer concentration and ionic strength. The pD reading of the D_2O buffers from the pH meter usually was 0.38–0.4 higher then that of the H_2O samples, and they were used without further adjustment. If necessary, NaOD and DCl solutions were used to alter the pD of the D_2O samples. ROS membranes used in the D_2O experiments were suspended in D_2O buffer for 2 h in the dark, which could allow the deuterons to replace the slowly exchanging protons from proteins. The membranes were then washed once with D_2O buffer by centrifugation before being used. Identical treatments were carried out in the H_2O samples as the controls. Purified proteins in 40% glycerol storage buffer were exchanged into D_2O buffer by means of a Bio-Rad P6 desalting column (0.5 cm × 5 cm) equilibrated with the D_2O buffer. All samples were kept at 4 °C during the experiments to avoid freezing of the D_2O buffer (pure D_2O has a freezing point of 4 °C). There is no significant difference in the stability of the photolyzed meta II rhodopsin in D_2O or H_2O buffers within the experimental time course (max 30 min) as monitored spectroscopically.

Rapid Quenching and Filtration Methods in Studying the Pre-Steady-State GTP Hydrolysis Reaction. The GTPase assays were performed in buffer B by measuring the release of [^{32}P]P_i from [γ-^{32}P]GTP (Fung & Stryer, 1980). The reaction mixture containing various amounts of transducin and ROS in 30 μL was photolyzed at 0 °C for 10 min. Reactions were initiated by the addition of 30 μL of 60 μM [γ-^{32}P]GTP. In the rapid-quenching experiments the reaction was stopped at the appropriate times by the addition of 0.2 M perchloric acid followed by molybdate precipitation. The inorganic phosphate molybdate precipitates were filtered onto Whatman glass fiber filters, and the radioactivity was counted. In the rapid filtration experiments, the reaction mixture was filtered at the appropriate times through a wetted nitrocellulose filter (Millipore type HA, 0.45-μm pore size). The filtrate was collected in a tube containing 0.2 M perchloric acid, and the amount of free [^{32}P]Pi was quantitated by molybdate precipitation using the same method as the rapid filtration experiments. Radioactivity associated with the protein that was bound onto the nitrocellulose filter was also quantitated.

Determination of the Single-Turnover Rate of P_i or GDP Release from T_α–GDP·P_i. The rate of P_i or GDP release from T_α–GDP·P_i was measured by a filtering-washing method (Navon & Fung, 1984). A reconstituted sample (30 μL) containing R* (30 μM) and T (10 μg) was mixed with 30 μL of excess [γ-^{32}P]GTP or [^{3}H]GTP (60 μM) at time = 0. The reaction mixture was allowed to incubate for 15 s, which was sufficient for the system to reach steady state. The reaction mixture was then diluted with 3 mL of buffer C and imme-

Scheme I

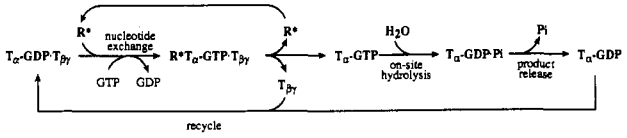

diately filtered through a nitrocellulose filter (Millipore type HA, 0.45-μm pore size). The filters were allowed to stand for various time intervals and then washed with 10 mL of ice-cold buffer C, and the radioactivity retained by the filter was measured.

Assays. Protein concentrations were determined by the Coomassie blue binding method (Bradford, 1976) using γ-globulin from Bio-Rad Laboratories as standard. PDE activity was monitored by the decrease of medium pH due to the hydrolysis of cGMP (Yee & Liebman, 1978). The reaction mixture contained 25 μM R*, 10 μg T, 20 μg PDE, and 5 mM cGMP in buffer D. Reactions were initiated by the addition of GTP or Gpp(NH)p. The change in pH in the reaction medium was monitored by a pH microelectrode (Microelectrodes Inc., Londonderry, NH) and a Radiometer PHM 82 pH meter. The results were recorded on a Soltex strip chart recorder. The change in pH was then converted to the amount of cGMP hydrolyzed.

RESULTS

Pre-Steady-State Kinetics Analyses

Partial Reactions of the Transducin Coupling Cycle. Transducin is a heterotrimer composed of three polypeptides, T_α (39 kDa), T_β (37 kDa), and T_γ (8.5 kDa), and acts as two functional subunits, T_α, and $T_{\beta\gamma}$. The T_α subunit is the activator of PDE. It contains a single guanine nucleotide binding site specific for GDP or GTP. Purified transducin in solution does not exchange its bound nucleotide nor hydrolyze GTP. The turnover of transducin requires the catalytic action of R*. The GDP-bound form of T_α has a high affinity for $T_{\beta\gamma}$ and R* and a low affinity for PDE. Interaction with R* opens the GTP-binding site on T_α for nucleotide exchange. Upon exchanging bound GDP for GTP, T_α–GTP dissociates from $T_{\beta\gamma}$ and R* and acquires a high affinity for PDE. The interaction of T_α with PDE activates the cGMP hydrolysis activity of PDE, which terminates when the T_α-bound GTP is hydrolyzed to GDP by the intrinsic GTPase activity associated with T_α. The GTP-binding site of dissociated T_α–GTP is in a closed conformation that prevents any further exchange reaction from occurring, thus committing the cascade cycle to operate unidirectionally. T_α must hydrolyze its bound GTP in order to return to its latent state and reassociate with $T_{\beta\gamma}$. After the release of P_i, T_α–GDP recombines with $T_{\beta\gamma}$, and the recycled $T_\alpha T_{\beta\gamma}$ complex is capable of binding and hydrolyzing additional GTP molecules in the presence of R*. The reaction cycle of transducin is depicted in Scheme I.

On the basis of our current understanding of the cGMP cascade, the first two steps of the transducin coupling cycle occur quickly in milliseconds time scale. The rates of the GTP/GDP exchange reaction and the dissociation of T_α–GTP and $T_{\beta\gamma}$ from the ROS membrane had been measured by light-scattering changes due to the release of the protein complexes from the disk membrane (Kuhn et al., 1981; Bennett & DuPont, 1985). These studies suggest that the exchange of guanine nucleotides and the dissociation of T_α–GTP occur in less than 100 ms. However, the turnover of the transducin molecule due to GTP hydrolysis was slow and occurs two to three times per minute. The slow turnover rate can be explained if one of the three remaining steps is rate limiting. These three partial reactions, the on-site hydrolysis of the tightly bound GTP, the release of the hydrolytic products P_i and GDP, and the recombination of deactivated T_α–GDP and $T_{\beta\gamma}$ for the initiation of another activation cycle, dictate the deactivation rate of transducin. It is necessary to examine each of the three reaction rates in order to provide a complete understanding of the dynamics of the transducin cycle.

Pre-Steady-State Kinetics Assayed by Rapid Quenching. To determine which of the last three partial reactions of the transducin cycle is rate limiting, we have conducted the following experiments. In preliminary studies, substituting H_2O with D_2O in the reaction buffer did not change the steady-state rate of GTP hydrolysis by transducin (Y.-K. Ho, D. T. Tobias, N. L.-F. Chang, and V. N. Hingorani, unpublished data). If the on-site GTP hydrolysis reaction is rate limiting, then one would expect to observe a primary isotope effect when D_2O is substituted for H_2O since the water molecule is one of the reactants in the hydrolysis reaction. The lack of a D_2O solvent isotope effect on the steady-state rate strongly suggests that the hydrolysis of GTP in Scheme I is not rate-limiting. The rate-limiting step may be the release of the hydrolysis product, P_i, or the reassociation of T_α–GDP with $T_{\beta\gamma}$. This can explain why a D_2O solvent isotope effect was not observed since these reactions do not involve the water molecule as a reactant. If the recombination of T_α–GDP with $T_{\beta\gamma}$ is rate limiting, a sizable fraction of transducin would then exist as T_α–GDP at steady state. Fung and Stryer (1981) have demonstrated that, in the R*-catalyzed GTP/GDP exchange reaction, all of the transducin-bound GDP were replaced by GTP and that GTP incorporation reached one mole of GTP per mole of transducin at steady state. We have repeated this experiment in the presence of excess R* and GTP and obtained the same result in which the guanine nucleotide binding site of transducin was saturated with GTP at steady state. This result suggests that the reassociation of T_α–GDP with $T_{\beta\gamma}$ occurs rapidly, and the recombined transducin complex can be immediately reactivated by R* without significant delay. These preliminary results indicate that the release of the hydrolytic product, P_i, may be the rate-limiting step of the transducin coupling cycle. If the rate of on-site GTP hydrolysis by T_α is faster than the rate of P_i release, an accumulation of T_α–GDP·P_i complexes will occur. One can then detect the formation of T_α-GDP·P_i by analyzing the pre-steady-state kinetics of the GTP hydrolysis reaction of transducin.

To study the kinetics of GTP hydrolysis and to detect the formation of T_α–GDP·P_i complexes, a rapid mixing and quenching system was used to monitor the rate of P_i formation. A sample containing transducin and excess R* was mixed rapidly with excess [γ-^{32}P]GTP at time zero. The presence of excess R* and [γ-^{32}P]GTP was essential to ensure that the incorporation of [γ-^{32}P]GTP into all of the nucleotide-binding sites of transducin was synchronized. The reaction mixture was then allowed to react for a predetermined time between 2 and 60 s. At the end of the incubation period, a third solution containing 0.2 M perchloric acid was rapidly added to the mixture to quench the reaction, and the amount of [^{32}P]P_i formed at each sample time point was quantitated by molybdate precipitation. As shown in Figure 1, the rate of P_i formation in the pre-steady-state is biphasic; it begins with a rapid phase from 1 to 4 s followed by a slow steady-state rate. This biphasic characteristic of P_i formation can be explained if the release of the hydrolytic product, P_i, is the rate-limiting step of the cycle. The rapid phase represents the formation of the T_α–GDP·P_i complex resulting from the fast on-site hydrolysis of bound GTP. The perchloric acid in the

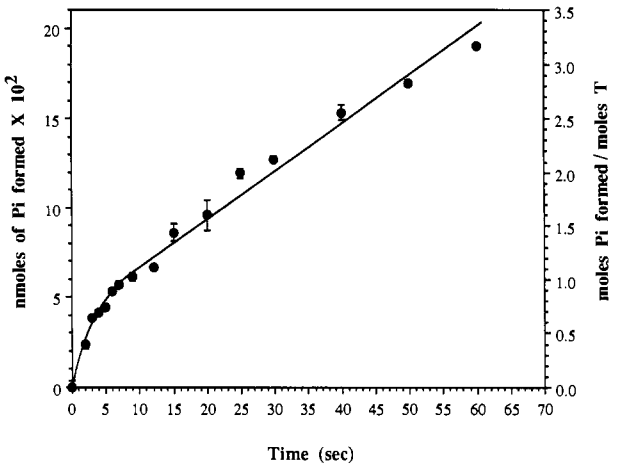

FIGURE 1: Results of the rapid-quenching experiments. Time course of P_i formation due to GTP turnover by transducin. A 30-μL solution containing 20 μM R* and 2 μM T (0.06 nmol) was mixed with a 30-μL solution containing 240 μM [γ-^{32}P]GTP at 22 °C at time = 0. The reaction was allowed to proceed for a predetermined period of time and subsequently quenched by the addition of 0.2 M perchloric acid. The data point at t = 0 was obtained by first quenching the reaction mixture of rhodopsin and transducin with perchloric acid prior to the addition of [γ-^{32}P]GTP. The amount of P_i formed was assayed by molybdate precipitation followed by radioactivity counting. Each data point represents the average of triplicate samples, and the error bar demonstrates the range of deviation.

quenching solution denatured the protein and released the tightly bound P_i, which can be detected as a "burst" of P_i formation. Since the breakdown of the T_α–GDP·P_i complex is slow, all the transducin molecules in the sample are rapidly transformed to the T_α–GDP·P_i form, and the continuous rise of the burst is stopped in approximately 4 s. As the tightly bound P_i is slowly released from T_α–GDP·P_i, the deactivated T_α–GDP recombines with $T_{\beta\gamma}$, which can enter another hydrolysis cycle. Thus, the slow phase of P_i formation represents the P_i release rate of the T_α–GDP·P_i complex and is the steady-state rate of GTP hydrolysis of the transducin cycle. The "burst" phenomenon in the pre-steady-state kinetics is similar to those observed in enzyme catalysis in which a covalent intermediate is involved, and the break-down rather than the formation of the intermediate is rate limiting. To analyze this "burst" phenomenon, some experimental parameters need to be defined. First, the rates of the on-site GTP hydrolysis and P_i release reaction steps can be obtained from the slope of the rapid and slow phases, respectively. Second, by extrapolating the slow steady-state rate toward the Y-axis at time = 0, a positive intercept can be obtained for quantitating the size of the initial burst. This intercept should be proportional to the amount of transducin present in the reaction mixture.[2] Third, by drawing two straight lines corresponding to the rapid and slow phases of the data, the intercept of these two lines define a transition point. On the basis of the proposed reaction scheme, the time required to reach this transition point represents the time required to activate all of the transducin molecules to the T_α–GDP·P_i form and is also the onset of the slow release of T_α-bound P_i. It is important to note that, after GTP is incorporated into transducin, the T_α–GTP complex dissociates from $T_{\beta\gamma}$ and the ROS membrane. The on-site GTP hydrolysis and the release of P_i are essentially unimolecular in nature and are the intrinsic properties of T_α alone. The size of the initial burst as calculated from Figure 1 is ~0.04 nmol of Pi. This represents 67% of the amount of T added (0.06 nmol). According to the equation in footnote 2, a ratio of 0.67 between the burst and amount of enzyme indicates that the rate of GTP hydrolysis is ~4.5 times higher than the rate of P_i release.

Pre-Steady-State Kinetics Assayed by Rapid Filtration. To confirm that the initial burst and the slow steady-state rate of P_i formation in the rapid-quenching experiments indeed represent the on-site GTP hydrolysis and the release of P_i from T_α–GDP·P_i, respectively, we have studied the pre-steady-state kinetics of GTP hydrolysis by rapid filtration methods. Similar to the rapid-quenching experiments, transducin and excess R* were mixed with [γ-^{32}P]GTP to initiate the reaction. After the incubation period, instead of acid quenching, the sample was diluted with a large volume of ice-cold buffer (3 mL) and filtered immediately through the nitrocellulose membrane. The dilution of the sample with cold buffer should prevent the recycling of the transducin due to a drop in temperature as well as the dilution of free [γ-^{32}P]GTP concentration. Moreover, the dilution to 3-mL volume facilitated the uniform filtering of the sample through the nitrocellulose membrane, which captured T_α–[γ-^{32}P]GTP and T_α–GDP·[^{32}P]P_i. The reaction mixture was then rapidly filtered through a vacuum filtration manifold onto nitrocellulose filters. The time between dilution and filtration was less than 2 s. The filtrate was collected and the appearance of free [^{32}P]P_i in the filtrate was quantitated via molybdate precipitation. Prior to filtration, the reaction mixture should contain four radioactive species, T_α–[γ-^{32}P]GTP, T_α–GDP·[^{32}P]P_i, the unreacted [γ-^{32}P]GTP, and the free [^{32}P]P_i released into solution. After filtration through the nitrocellulose filter, the T_α–[γ-^{32}P]GTP and T_α–GDP·[^{32}P]P_i species will be retained on the nitrocellulose filter, whereas the [γ-^{32}P]GTP and [^{32}P]P_i will be in the filtrate. By this method, the T_α-bound [^{32}P]P_i in the form of T_α–GDP·[^{32}P]P_i can be separated from free [^{32}P]P_i. The rate of the appearance of free [^{32}P]P_i assayed by the rapid filtration method is shown in Figure 2. The production of free [^{32}P]P_i from the GTPase activity of transducin has an initial lag of ~4–6 s followed by an increased steady-state rate. This observation confirms the interpretation of the results from the acid-quenching experiments. As described above, the initial burst in the acid quenched experiments is due to the on-site hydrolysis of the T_α-bound [γ-^{32}P]GTP, which leads to the formation of the T_α–GDP·[^{32}P]P_i complex. Since T_α–GDP·[^{32}P]P_i is not denatured in the rapid filtration experiments and is retained on the nitrocellulose filter, filtrates from the initial time points should not contain free [^{32}P]P_i. As a result, the appearance of free [^{32}P]P_i shows an initial lag that corresponds to the initial burst in the acid-quenching experiments. After the initial lag, the [^{32}P]P_i formation follows a steady rate that is due to the release of T_α-bound [^{32}P]P_i and the turnover of transducin molecules. This steady-state rate should be equivalent to the slow phase of the acid-quenched experiments, and, within experimental error, they are indeed the same. In addition to monitoring the free [^{32}P]P_i in the filtrate, the radioactivity associated with the nitrocellulose filter at each time point was also assayed. The nitrocellulose filter should trap the T_α–[γ-^{32}P]GTP and T_α–GDP·[^{32}P]P_i complexes. Since the incorporation of [γ-^{32}P]GTP occurs in <1 s and the trapped radioactivity on the filter cannot be used to distinguish T_α–[γ-^{32}P]GTP from T_α–GDP·[^{32}P]P_i, the ra-

[2] The magnitude of the burst is proportional to transducin concentration and is related to the rate of the GTP hydrolysis and P_i release reactions according to

$$\pi = k_{+2}^2 e_0/(k_{+2} + k_{+3})^2$$

where π is the magnitude of the burst, k_2 and k_3 are the rate constants for the GTP hydrolysis and P_i release reactions, respectively, and e_0 is the transducin concentration (Cornish-Bowden, 1976).

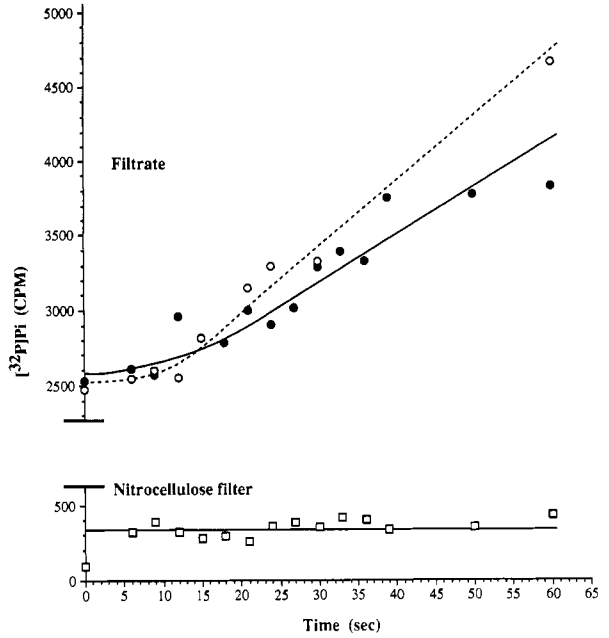

FIGURE 2: Results of the rapid filtration experiments. Time course of free P_i formation due to GTP turnover by transducin. A 30-μL solution containing 12 μM R* and 1.2 μM T was mixed with a 30-μL solution containing 60 μM [γ-^{32}P]GTP to initiate the reaction. The reaction was allowed to incubate at 22 °C for a predetermined period. At the end of the incubation, the sample was diluted with a large volume of ice-cold buffer and immediately filtered through a vacuum filtration manifold onto nitrocellulose filters. The data point at t = 0 was obtained by first diluting the reaction mixture of rhodopsin and transducin with a large volume of ice-cold buffer prior to the addition of [γ-^{32}P]GTP. The filtrate was collected and the appearance of free [^{32}P]P_i in the filtrate was quantitated via molybdate precipitation. The results of two independent sets of experiments are shown by ● (solid line) and ○ (dotted line), which represent the amount of free [^{32}P]P_i present in the filtrate as assayed by molybdate precipitation. (□) The [^{32}P] radioactivity associated with proteins, T_α–[γ-^{32}P]GTP and T_α–GDP·[^{32}P]P_i, which were bound on the nitrocellulose filter. Each data point represents the average of duplicate samples.

dioactivity associated with the filter should remain constant throughout the entire time course of the measurement. The amount of radioactivity trapped on the filter during the initial lag period is identical with that obtained at the steady state (Figure 2). It is likely that, during the initial lag phase, the transducin molecules retained on the nitrocellulose filter are a mixture of T_α–[γ-^{32}P]GTP and T_α–GDP·[^{32}P]P_i. Similarly, during the steady-state phase, they are mainly in the form of T_α–GDP·[^{32}P]P_i. Results from these two complementary methods of analyzing the pre-steady-state kinetics provide a definitive interpretation of the pre-steady-state kinetics of GTP-hydrolysis by transducin.

Quantitative Analyses of the Pre-Steady-State Kinetics

The biphasic characteristic of the pre-steady-state kinetics of GTP hydrolysis assayed by the rapid acid-quenching method has provided a means to measure independently the rates of the two partial reactions of the transducin cycle, the on-site GTP hydrolysis and the release of the hydrolytic product, P_i. The preliminary data of Figure 2 indicate that the on-site hydrolysis rate is approximately 4 times faster than the rate of release of the tightly bound P_i. To eliminate the possibility that the observed biphasic characteristic is due to nonspecific hydrolysis of GTP introduced in the rapid-mixing and acid-quenching procedures, we have carried out a series of experiments to analyze the pre-steady-state kinetics quantitatively. it is important to mention that the rapid mixing in all the experiments was carried out manually. The fastest time point

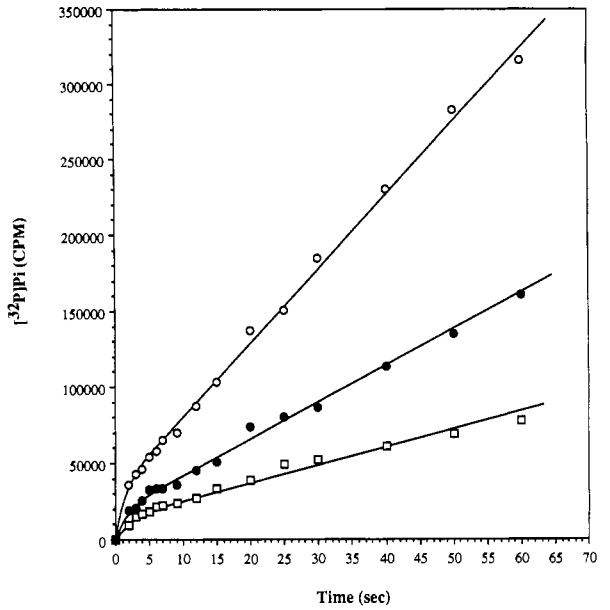

FIGURE 3: Effect of transducin concentration on the pre-steady-state kinetics of GTP hydrolysis. The GTPase assays were carried out at 22 °C according to the rapid-quenching protocol. The reaction volume was 60 μL, and each sample contained 120 μM [γ-^{32}P]GTP and excess R* (20 μM) and various amounts of T: (□) 1 μM, (●) 2 μM, and (○) 4 μM.

that provided reliable data was 2 s. Thus, we are lacking accurate data on the GTP/GDP exchange rate, which is assumed to occur in <1 s. The quantitative analyses described below serve as an internal control for the rapid-quenching experiments. The results ensure the correct interpretation of the kinetic data and also provide an in-depth understanding of the biochemistry and molecular dynamics of the transducin coupling cycle.

Effect of Transducin Concentration. The initial burst of P_i formation in the rapid-quenching experiments was interpreted as the accumulation of T–GDP·P_i complexes. Therefore, increasing transducin concentration should have a corresponding increase on the size of the initial burst. Similarly, increasing transducin concentration should also increase the steady-state rate of GTP hydrolysis as well as the rate of the slow phase of P_i production. As noted above, the on-site GTP hydrolysis and the release of P_i are intrinsic properties of T_α and are essentially unimolecular in nature. Hence, the time required for the T_α-bound GTP to be hydrolyzed and the time T_α retains the hydrolytic products before releasing them to solution should be independent of transducin concentration, so that, at a given temperature, an increase in transducin concentration should not affect the time required to reach the transition point. The effect of increasing transducin concentration on the pre-steady-state kinetics of GTP hydrolysis is shown in Figure 3. The results are in complete agreement with the predictions described above. As the transducin concentration increases, proportional increases in the rates of on-site GTP hydrolysis, P_i release, and the intercept representing the size of the initial burst were observed. However, the time required to reach the transition point between the rapid and slow phases remained constant at ~4–6 s.

Role of T_α and T_β. The binding of transducin to R* requires the cooperative interaction between the T_α and $T_{\beta\gamma}$ subunits (Fung, 1983). Individual T_α or $T_{\beta\gamma}$ do not bind well to R*. However, maximum binding can be achieved when T_α and $T_{\beta\gamma}$ are present in a 1:1 ratio as they are in ROS. This indicates that the formation of the $T_\alpha T_{\beta\gamma}$ heterotrimer is essential for high-affinity binding to R*. $T_{\beta\gamma}$ apparently plays an important

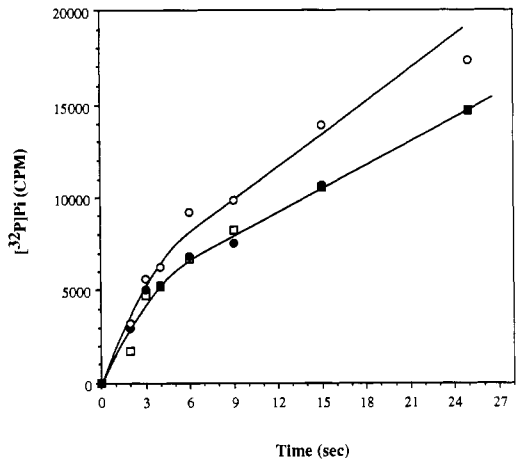

FIGURE 4: Effect of purified subunits of transducin on the pre-steady-state kinetics of GTP hydrolysis. The GTPase assays were carried out at 22 °C according to the rapid-quenching protocol. Each sample contained 6 μM R*, 0.6 μM T, and 30 μM [γ-^{32}P]GTP in a volume of 60 μL. The control samples (□) contained no additional transducin subunits. The T_α samples (○) also contained 0.5 μg/μL T_α in addition to the 0.6 μM of T in the reaction mixture. The $T_{\beta\gamma}$ samples (●) contained an addition of 0.5 μg/μL $T_{\beta\gamma}$.

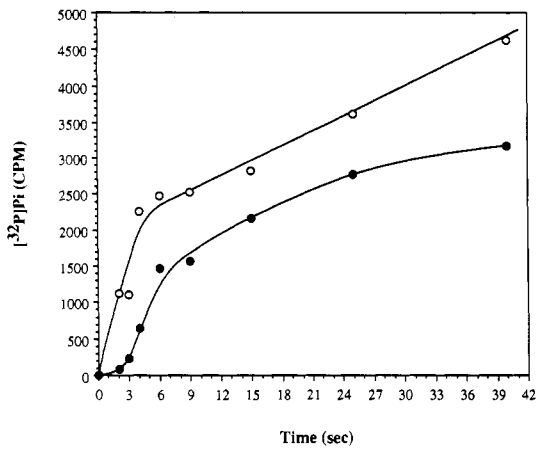

FIGURE 5: Effect of nonhydrolyzable GTP analogue on the pre-steady-state kinetics of GTP hydrolysis. The GTPase assays were carried out at 22 °C according to the rapid-quenching protocol. Each sample contained 6 μM R*, 0.6 μM T, and 30 μM [γ-^{32}P]GTP in a volume of 60 μL. The effect on the GTPase activity with no Gpp(NH)p (○) added and with 10 μM Gpp(NH)p (●) is shown.

role in presenting T_α to R*, however, it does not participate in the GTP hydrolysis or the P_i release steps as depicted in Scheme I. The dissociated $T_{\beta\gamma}$ recycles quickly with T_α to form another $T_\alpha T_{\beta\gamma}$ complex capable of binding additional GTPs in the presence of R*. Conversely, the dissociated T_α–GTP does not turnover as quickly as $T_{\beta\gamma}$. It has to hydrolyze the bound GTP and slowly release the bound P_i before T_α–GDP can recombine with $T_{\beta\gamma}$. As a result, in the presence of excess R* and GTP, T_α becomes the limiting factor that controls the GTPase activity of transducin. Although the binding of $T_\alpha/T_{\beta\gamma}$ to R* requires a 1:1 ratio, $T_{\beta\gamma}$ functions catalytically in turnover over the GTPase activity of T_α, i.e., the maximal GTPase activity can be attained with an amount of $T_{\beta\gamma}$ that is considerably less than that of T_α (Fung, 1983). Therefore, excess $T_{\beta\gamma}$ over T_α should not significantly increase the GTPase activity of transducin. In a reconstituted system, the ratio of T_α to $T_{\beta\gamma}$ can be altered easily by incorporating additional T_α or $T_{\beta\gamma}$ to the system, and their effect on the pre-steady-state kinetics is shown in Figure 4. Increasing the T_α concentration above a 1:1 ratio to $T_{\beta\gamma}$ showed corresponding increases in the initial burst as well as the steady-state rate of GTP hydrolysis. This indicates that the $T_{\beta\gamma}$ present in the system is sufficient to facilitate the GTP/GDP exchange reaction of the added purified T_α. As a result, more T_α–GDP·P_i accumulated and was detected as an increase of the initial burst. Conversely, increasing $T_{\beta\gamma}$ concentration over the 1:1 ratio with T_α had little effect on the pre-steady-state kinetics. This result serves as a control to corroborate conclusions drawn from the above studies. Furthermore, increasing transducin concentration or purified T_α and $T_{\beta\gamma}$ subunits did not alter the time required to reach the transition point. If the rate-limiting step of the transducin cycle is the reassociation of the transducin subunits, increasing transducin concentration should have reduced the time for reaching the transition point. This observation argues for the rate-limiting step of the transducin coupling cycle as being the release of tightly bound P_i from T_α–GDP·P_i.

Effect of Nonhydrolyzable GTP Analogue. Nonhydrolyzable analogues of GTP, such as Gpp(NH)p and GTPγS, have been used as competitive inhibitors of the GTPase activity of transducin. Although they inhibit GTP hydrolysis, they were found to be equally effective in dissociating T_α and $T_{\beta\gamma}$ and in activating the latent PDE. These observations indicate that the on-site hydrolysis of GTP is not an essential requirement for transducin subunit dissociation or for inducing the conformational change that leads to PDE activation. The effect of Gpp(NH)p on the pre-steady-state kinetics of GTP hydrolysis was examined. The results are shown in Figure 5. In general, the results are as expected. Gpp(NH)p reduces the initial burst and inhibits the steady-state rate. Upon further inspection of the data, additional features of the effect of Gpp(NH)p are revealed. First, the transition between the initial burst and the slow steady-state rate is not as distinct as the control. Second, the inhibition by Gpp(NH)p progresses gradually. Gpp(NH)p has less effect on the initial rate; however, as hydrolysis approaches steady state, the inhibition increases and eventually shuts off GTP hydrolysis. This result is unique to the transducin cycle. Although Gpp(NH)p is a competitive inhibitor of GTP, it functions kinetically as a dead-end inhibitor due to the fact that T_α–Gpp(NH)p dissociates from $T_{\beta\gamma}$ and R* and its nucleotide-binding site is in a closed conformation. The bound Gpp(NH)p is no longer in equilibrium with free nucleotides in solution, and as a result T_α–Gpp(NH)p remains dissociated from $T_{\beta\gamma}$ and R* and becomes a dead-end complex. The gradual inhibition by Gpp(NH)p as shown in Figure 5 can be explained in the following terms. In the initial period, Gpp(NH)p competes with GTP for binding to transducin, which results in a fraction of the transducin population being inhibited by Gpp(NH)p by forming the T_α–Gpp(NH)p complex. The remaining active transducin molecules recycle after the hydrolysis of the bound GTP, which generates a small initial burst. As the reaction approaches steady state, additional transducin molecules are inhibited by Gpp(NH)p binding, and the majority of T_α are gradually tied up by Gpp(NH)p. Hence, the GTPase activity becomes abolished over time. This observation is in complete agreement with the current knowledge of the transducin cycle. It is important to point out that although GTP hydrolysis was observed at pre-steady-state, the concentration of Gpp(NH)p used in the experiment was sufficient to completely inhibit GTP hydrolysis at steady state assayed after 3 min of incubation.

Temperature Dependence. The temperature dependence of the pre-steady-state kinetics of GTP hydrolysis was investigated between 4 and 40 °C. The results are shown in Figure 6. As expected, the reaction rates generally increase with

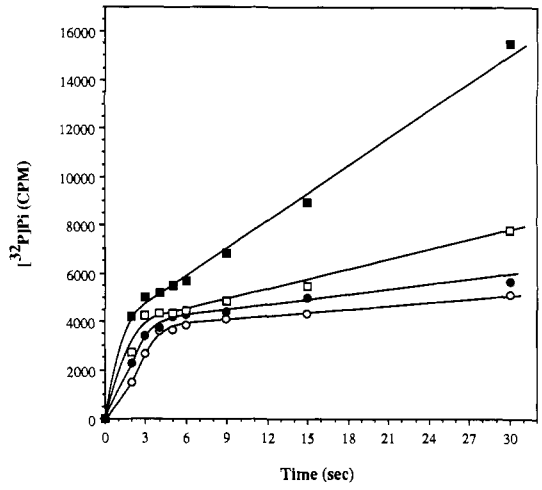

FIGURE 6: Effect of temperature on the pre-steady-state kinetics of GTP hydrolysis. The GTPase assays were carried out at various temperatures according to the rapid-quenching protocol. Each sample contained 6 μM R*, 0.6 μM T, and 30 μM [γ-^{32}P]GTP in a volume of 60 μL. The various temperatures are 4 (○), 10 (●), 22 (□), and 38 (■) °C.

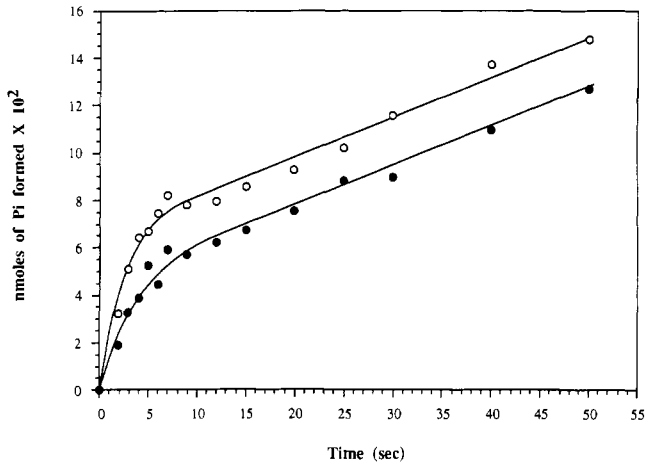

FIGURE 7: D_2O solvent isotope effect of the pre-steady-state kinetics of GTP hydrolysis. The GTPase assays were carried out at 22 °C according to the rapid-quenching protocol. The H_2O (○) and D_2O (●) samples are prepared as described under Experimental Procedures. Each sample contained 9 μM R*, 0.9 μM T, and 30 μM [γ-^{32}P]GTP in a volume of 60 μL in their respective buffers. Each data point represents the average of quadruplet samples.

increasing temperatures. Both the initial rates of the on-site GTP hydrolysis and the steady-state rate of P_i release increase with respect to increasing temperature. In addition, several implications can be deduced from the temperature-dependence study. (1) Despite an increase of the initial rate of P_i formation at higher temperatures, the size of the initial burst at different temperatures remains unchanged. As discussed above, the magnitude of the initial burst is related mainly to transducin concentration. Since all samples contained the same amount of transducin, the size of the initial burst should remain the same. The observation of the biphasic kinetics at all temperatures also implies that P_i release remains the rate-limiting step of the transducin coupling cycle. Temperature does not alter the mode of action of transducin. (2) The time required to reach the transition point between the initial burst and the slow steady-state rate increases as temperature decreases. As described in Figure 3, this transition is related to the intrinsic properties of the T_α–GTP complex. The rates of on-site GTP hydrolysis as well as the release of P_i from T_α are slowed down at lower temperatures, and the system requires more time to reach the steady-state rate. (3) It is important to point out that at low temperature (4–10 °C), a short time lag can be detected before the initial burst is observed. This lag may be due to decreases in the rates of the first two partial reactions of the transducin cycle as described in Scheme I. The lag encompasses the time required for the GTP/GDP exchange reaction that formed T_α–GTP and the time for T_α–GTP to exist before the on-site GTP hydrolysis occurs. The formation of T_α–GDP·P_i is then detected as the initial burst in the acid-quench experiments. (4) The temperature dependence of the two partial reactions detected in the acid-quench experiments are different. At temperatures below 10 °C, the initial burst is easily detected, indicating that the on-site GTP hydrolysis still proceeds at a relatively fast rate. However, the steady-state rate of P_i release has diminished significantly at low temperatures. To quantitate this observation, the temperature dependence of the two partial reactions is analyzed by the Arrhenius plot of reaction rate vs inverse temperature. Both partial reactions exhibited linear Arrhenius plot. The results indicate that the rate of the on-site GTP hydrolysis reaction exhibits less temperature dependence with an activation energy (E_a) of 28.1 kJ per mole of GTP hydrolyzed, the release of P_i from T_α–GDP·P_i is more temperature dependent with an estimated E_a of 44.7 kJ per mole of P_i released (data not shown). Results from the temperature studies provide further support to the interpretation of the kinetic data. Furthermore, it clearly demonstrates that the two partial reactions of transducin GTPase activity can be studied independently by the pre-steady-state method.

D_2O Solvent Isotope Effect. We have carried out preliminary experiments to study the D_2O solvent isotope effect on the activation of the retinal cGMP cascade and found that the steady-state GTPase activity of transducin had no D_2O solvent isotope effect (Y.-K. Ho, D. T. Tobias, N. L.-F. Chang, and V. N. Hingorani, unpublished data). The steady-state rate of GTP hydrolysis was the same in D_2O and in H_2O. We proposed that this observation is due to the rate-limiting step in the reaction path of the GTPase activity as being the release of P_i from T_α–GDP·P_i but not the on-site hydrolysis of GTP. The pre-steady-state kinetics analyses allow us to confirm this interpretation. Since a water molecule directly participates in the on-site GTP hydrolysis step as a reactant, a primary isotope effect may be observed in the initial burst of the pre-steady-state kinetics. However, water molecules may not participate in the slow step of P_i release; thus the steady-state rate of the GTPase activity may remain unchanged in H_2O and D_2O buffers. The effect of D_2O on the pre-steady-state kinetics is shown in Figure 7. The initial rise of the rapid phase is slower in D_2O buffer with a solvent isotope effect of approximately 1.7, while no solvent isotope effect can be detected in the steady-state rate. These results are in complete agreement with the above scheme. The size of the initial burst is smaller in D_2O buffer, and the time required to reach the transition point is also slightly longer. These observation can be explained in the following terms. Since bound GTP is hydrolyzed slower in D_2O buffer during the initial burst, less T_α–GDP·P_i is formed than in the H_2O sample. As a result, the size of the burst is smaller. Similarly, the slower rate of the on-site GTP hydrolysis in D_2O results in a longer time period to reach the transition point. However, once the system reaches the steady state, further GTP hydrolysis is limited by how fast the tightly bound P_i can be released, which is the same in H_2O and D_2O.

Role of T_α–GDP·P_i in PDE Activation

Pre-steady-state kinetic analyses described above indicate that P_i release from T_α–GDP·P_i is the rate-limiting step of the

transducin coupling cycle. The slow turnover of T_α–GDP·P_i leads to the accumulation of T_α–GDP·P_i, which becomes the most abundant species in the system at steady state. Several questions concerning the activation of PDE by transducin can be raised in light of this implication. Does T_α–GDP·P_i have the same conformation as T_α–GTP? Is T_α–GDP·P_i capable of activating PDE? Which of the partial reactions, the on-site GTP hydrolysis or the release of P_i from T_α–GDP·P_i, actually control the deactivation of transducin? Answers to these questions will have significant consequence in the dynamics of the cGMP cascade. It has been shown that the light-activated PDE activity can be turned off in less than 2 s under physiological conditions (Sitaramayya & Liebman, 1983). if T_α–GDP·P_i is capable of activating PDE, its long half-life in the order of 20 s will make the deactivation of transducin so slow as to preclude it from being the major turn-off mechanism for the cGMP cascade. This may mean that the cGMP cascade is shut off via other mechanisms such as the phosphorylation of R* or an increase in guanylyl cyclase activity to compensate for the cGMP hydrolyzed by PDE. However, if T_α–GDP·P_i is incapable of activating PDE, it would imply that the rapid on-site hydrolysis of the T_α-bound GTP may function as the deactivation step for transducin. Since on-site GTP hydrolysis occurs between 100 ms and 3 s, the hydrolysis of GTP by transducin may play a significant role in shutting off the cascade. In order to gain some insight to these questions, we conducted experiments comparing the rate of P_i release from T_α–GDP·P_i and the rate of PDE deactivation associated with the turnover of transducin. If these two rates are similar, then the first possibility discussed above is correct, and T_α–GDP·P_i is capable of activating PDE and the deactivation of transducin is controlled by the release of the tightly bound P_i. If the rate of PDE deactivation is much faster than the rate of P_i release, then the deactivation of transducin is associated with the on-site hydrolysis of T_α-bound GTP.

Rate of PDE Deactivation. The rate of PDE deactivation associated with the turnover of transducin can be measured in a system containing R*, purified T, PDE, and excess cGMP (5 mM) (Frey et al., 1988). A pH electrode was used to monitor the PDE activity, which can be detected as a decrease in medium pH due to cGMP hydrolysis. The results are shown in Figure 8A. In the absence of GTP, PDE remained latent and no activity was detected. When a limited amount of GTP (0.3 μM) was added at time zero to initiate the reaction, PDE activity increased but slowly diminished back to the basal level. This is due to the turnover of transducin's GTPase activity consuming all the added GTP. From the decay curve of PDE activity, the value for the ratio of (GTP_t/GTP_0) can be determined at various time points for kinetic analysis. GTP_0 represents the total amount of GTP in the reaction mixture at time = 0, whereas GTP_t represents the amount of GTP remaining at time = t. The decay process follows pseudo-first-order kinetics. A linear plot of ln (GTP_t/GTP_0) vs time is obtained as shown in Figure 8B. The slope of the linear plot corresponds to the first-order rate constant of 0.0180 s^{-1} for the deactivation of PDE.

Rate of P_i Release from T_α–GDP·P_i. The rate of P_i release from T_α–GDP·P_i was measured by a filtering-washing method (Navon & Fung, 1984). A reconstituted sample containing R* and transducin was mixed with excess [γ-^{32}P]GTP (30 μM) at time = 0. The reaction mixture was allowed to incubate for 15 s which was sufficient for the system to reach steady state. At this time, all the transducin should be activated forming the T_α–GDP·[^{32}P]P_i complex. The reaction mixture was then diluted with buffer and immediately filtered

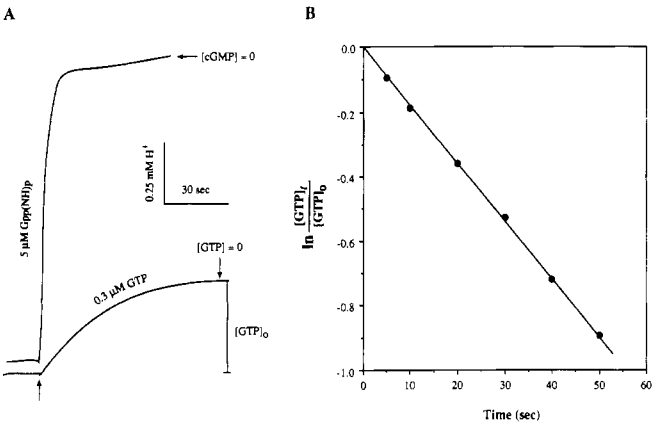

FIGURE 8: Rate of PDE deactivation associated with the turnover of transducin. The reactions were carried out at 22 °C as described under Experimental Procedures. Each sample contained 25 μM R*, 10 μg T, 20 μg PDE, and 5 mM cGMP. The reactions were initiated by the addition of 0.3 μM GTP or 5 μM Gpp(NH)p. (A) Results of the PDE activation assay as monitored by the rate of H^+ release due to cGMP hydrolysis using a pH electrode. The arrow indicate the addition of GTP or Gpp(NH)p. Total hydrolysis of the cGMP in the reaction mixture is shown by the top curve where the cascade was activated by the addition of nonhydrolyzable Gpp(NH)p. The bottom curve represents the deactivation of PDE activity due to the hydrolysis of bound GTP by transducin. (B) First-order kinetic plot of the rate of PDE deactivation due to the hydrolysis of GTP. The values of GTP_t and GTP_0 are determined from the experimental trace of the PDE assays described for panel A. GTP_0 represents the total GTP content in the reaction mixture at time 0, and GTP_t represents the amount of GTP remaining at time t. Hence, GTP_t/GTP_0 represents the fraction of GTP remaining at time t. The value of the slope of the linear plot of ln (GTP_t/GTP_0) vs time is used to calculate the first-order rate constant of PDE deactivation.

through a nitrocellulose filter. T_α–GDP·[^{32}P]P_i was retained by the filter, whereas excess [γ-^{32}P]GTP and free [^{32}P]P_i were removed into the filtrate. The lack of [γ-^{32}P]GTP on the filter limited any further GTP/GDP exchange reactions. However, the T_α–GDP·[^{32}P]P_i complex associated on the moistened nitrocellulose remained active and slowly released the tightly bound P_i. The nitrocellulose filters containing T_α–GDP·[^{32}P]P_i were allowed to stand for various time intervals and then washed with 10 mL of ice-cold buffer to remove any free [^{32}P]P_i released from T_α–GDP·[^{32}P]P_i. Thus, the decrease of radioactivity associated with the nitrocellulose filters as a function of the time between the loading T_α–GDP·[^{32}P]P_i onto the filter and the removal of free [^{32}P]P_i by washing the filter should represent the rate of P_i release from the T_α–GDP·[^{32}P]P_i complex. This method monitors the single-turnover rate of the T_α–GDP·P_i complex. The results are shown in Figure 9. Again the [^{32}P]P_i release rate follows first-order kinetics. A linear plot of ln (P_t/P_0) vs time can be used to determine the rate constant for the release of P_i from T_α–GDP·P_i (where P_0 represents the radioactivity associated with the filter at time = 0 and P_t is the radioactivity remaining on the filter at time = t after washing the filter with buffer). The slope of the linear plot corresponds to the first-order rate constant of 0.0173 s^{-1} for P_i release from T_α–GDP·P_i.

As can be seen, the rates of PDE deactivation and P_i release are the same within experimental error. This comparison conclusively demonstrates that the release of tightly bound P_i from T_α–GDP·P_i is the deactivation step of transducin. The fact that the decay of PDE activity follows first-order kinetics implies that T_α–GTP and T_α–GDP·P_i have similar conformations and both have the ability to activate PDE. If T_α–GTP and T_α–GDP·P_i activate PDE with different kinetics, one may observe biphasic decay kinetics in PDE activity with one phase corresponding to the on-site hydrolysis of T_α-bound GTP and

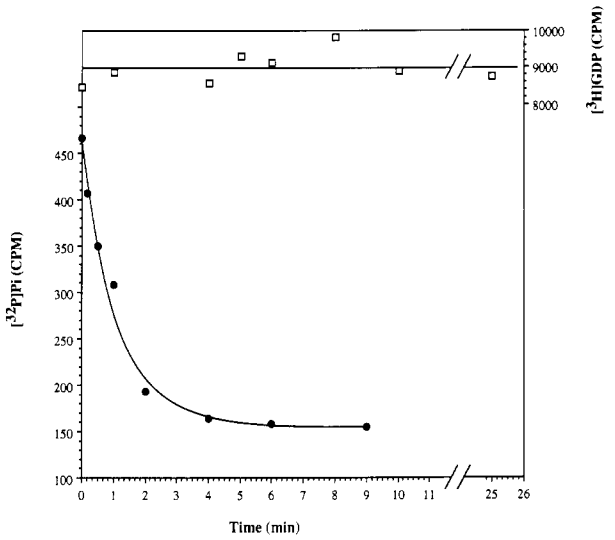

FIGURE 9: Results of the experiments measuring the rate of GDP and P_i release from T_α–GDP·P_i. A 30-μL sample containing 30 μM R* and 10 μg T was mixed with 30 μL of excess [γ-^{32}P]GTP or [^{3}H]GTP (60 μM) at time = 0. The reaction was allowed to reach steady state and subsequently filtered through a nitrocellulose filter. The filters were incubated for various time intervals and washed again with buffer. The radioactivity retained by the filter was then counted. (●) The time course of P_i release from T_α–GDP·P_i as measured by using [γ-^{32}P]GTP to monitor [^{32}P]P_i release from T_α–GDP·P_i. (□) The time course of GDP release from T_α–GDP·P_i as measured by using [^{3}H]GTP to monitor [^{3}H]GDP release.

the other to the release of the tightly bound P_i. Judging from the slow deactivation rate of PDE as regulated by transducin GTPase activity, one must conclude that the retinal cGMP cascade would most likely be turned off by other processes such as R* phosphorylation and guanylyl cyclase activity enhancement, which occur in a faster time scale under physiological conditions.

Formation of a Stable T_α–GDP Complex. After releasing the tightly bound P_i, T_α–GDP resumes an inactive conformation and recombines with $T_{\beta\gamma}$ to be ready for another R*-catalyzed activation cycle. The stability of the T_α–GDP complex and whether GDP is released from T_α–GDP can be deduced by the following experiments. The techniques employed in the experiments measuring the single-turnover rate of P_i release from T_α–GDP·P_i can also be used to study the release of tightly bound GDP. With [^{3}H]GTP as the radioactive tracer, the rate of [^{3}H]GDP release from T_α–[^{3}H]-GDP·P_i was measured, and the results are shown in Figure 9. [^{3}H]GDP remains tightly bound to T_α for more than 20 min. This observation implies that T_α–GDP is a very stable complex and GDP is never released from T_α–GDP leaving an empty nucleotide-binding site. The nucleotide-binding site of T_α–GDP may be in a closed conformation that holds tightly onto the bound GDP, which can only be released via the GTP/GDP exchange reaction in the presence of GTP, $T_{\beta\gamma}$, and R*.

Effect of PDE and Arrestin. The physiological role of T_α–GTP is to activate the latent PDE. To study whether the interaction of T_α–GTP with the inhibitory P_γ peptide of PDE increases the turnover rate of transducin, purified PDE was added to the reconstituted system containing R* and transducin, and the effect on the pre-steady-state kinetics of GTP hydrolysis was analyzed. Although the molar ratio of PDE and transducin in ROS has been estimated to be approximately 1:10, equimolar PDE and transducin was used to ensure that every transducin molecule would have a chance to interact with PDE. Under these experimental conditions, PDE was activated by transducin in the presence of GTP up to 75% of the trypsin-activated level. However, as shown in Figure 10A, the addition of PDE had no effect on the pre-steady-state kinetics of GTP hydrolysis by transducin. This observation implies that the binding of GTP to the T_α nucleotide-binding site exposes the effector-binding site on T_α and enhances the interaction with PDE for activation, but the binding of PDE to the effector-binding site of T_α has no reverse effect on GTP hydrolysis. As mentioned above, the coupling cycle of transducin proceeds unidirectionally due to the dissociation of T_α–GTP from $T_{\beta\gamma}$ and R*, and the interaction with PDE has no direct feedback regulation on the transducin coupling cycle. This unidirectional coupling may represent a special feature of G-protein mediated signal transducin systems. The 48-kDa protein, or arrestin, binds to phosphorylated R* and quenches its capacity to activate transducin and PDE (Wilden et al., 1986). To study whether arrestin may directly interact

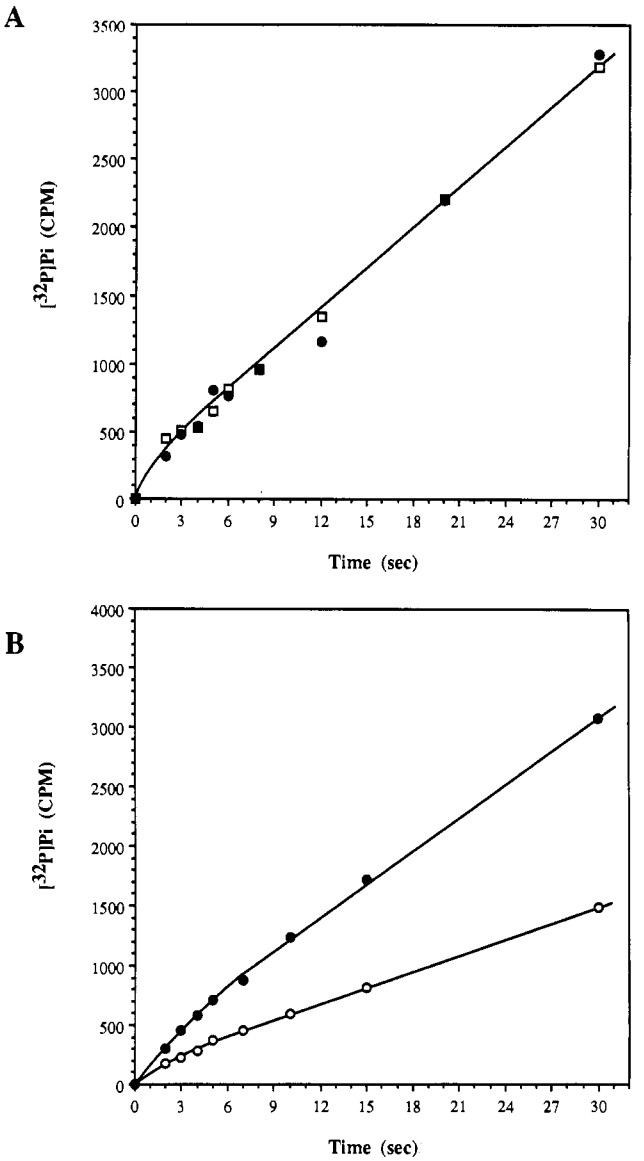

FIGURE 10: Effect of PDE and FITC modification of T_α on the rate of P_i formation. The GTPase assays were carried out at 22 °C according to the rapid-quenching protocol. (A) The effect of PDE. Each sample contained 6 μM R*, 0.6 μM T, and 30 μM [γ-^{32}P]GTP in a volume of 60 μL. The effect on the GTPase activity with no PDE (●) and 0.33 μg/μL PDE (□) is shown. (B) The effect of FITC modification of T_α. T_α was modified with FITC according to the method of Hingorani and Ho (1987). Each sample contained 6 μM R*, 30 μM [γ-^{32}P]GTP in a volume of 60 μL with either 0.5 μg/μL unmodified T (●), or 0.5 μg/μL FITC-modified T (○).

with transducin and alter the GTP hydrolysis activity, purified arrestin with molar ratio of 1:1 to transducin was added to the reconstituted system containing purified R* and T, and the effect on the pre-steady-state kinetics of GTP hydrolysis was studied. Similar to the results of adding PDE, arrestin in the absence of phosphorylated R* demonstrated no effect on the transducin GTP activity (data not shown). This observation is in compliance with the precept that arrestin's inhibitory role is to compete with transducin for binding to phosphorylated R* and not to inhibit transducin through direct interactions.

Effect of FITC Modification of T_α. Many chemical modifications of transducin have been shown to diminish its R*-catalyzed GTPase activity. This inhibition may be due to one or a combination of three possibilities. (i) The modification may be interfering with the interaction among T_α, $T_{\beta\gamma}$, and R* that blocks the GTP/GDP exchange reaction. (ii) The modification may eliminate certain functional groups required for the catalysis of the GTP hydrolysis reaction at the nucleotide-binding site. (iii) The modification may have no effect on the GTP hydrolysis reaction but retard P_i release from the T_α–GDP·P_i complex, which slows down the turnover rate of T_α–GDP·P_i. An inhibition of T/R* interaction can be easily detected by assaying the binding of transducin to rhodopsin membrane. In the case of sulfhydryl modification with *N*-ethylmaleimide, the inhibition of the GTPase activity of transducin had been suggested to be due to the inhibition of T/R* interaction (Ho & Fung, 1984). It has been difficult to distinguish which of the latter two possibilities may be responsible for the inhibition of transducin's GTPase activity. The pre-steady-state kinetic analyses introduced in this study can be used as a method for studying the two reactions of GTP hydrolysis and P_i release separately. This will provide new insights on inhibitory mechanisms. Modification of a single lysine residue to T_α by fluorescein 5′-isothiocyanate (FITC) (Hingorani & Ho, 1987) had been shown to diminish the steady-state GTPase activity of transducin while having no effect on the GTP/GDP exchange reaction. The fact that GTP can be incorporated into T_α indicates that FITC modification did not block the interaction between transducin and R*. This implies that the inhibition must due to one or both of the latter two possibilities. The effect FITC modification of T_α has on the pre-steady-state kinetics of GTP hydrolysis was examined by the rapid-quenching method, and the results are shown in Figure 10B. The biphasic characteristic of P_i formation of FITC-modified transducin is greatly diminished. Both the magnitude of the initial burst and the steady-state rate are also reduced. This result suggests that FITC modification inhibits both the rate of on-site GTP hydrolysis as well the release of tightly bound P_i, and no distinct rate-limiting step can be determined from these studies. This interpretation explains why both the initial burst and steady-state rate are decreased.

Discussion

Results from this work suggest that, during the course of GTP hydrolysis by transducin, stable T_α–GDP·P_i complexes are formed that possess a conformation similar to T_α–GTP and are capable of activating PDE. Thus, transducin is not deactivated when the T_α-bound GTP is hydrolyzed. The rate of deactivation is limited by the rate of the release of the tightly bound P_i from T_α–GDP·P_i. This rate is approximately 4–5 times slower than that of the on site hydrolysis of GTP. The difference between these two rates suggests that T_α–GTP exists only as a transient species at the initial stage of activation. As the process approaches steady state, T_α–GDP·P_i accumulates and functions as the major species that activates the latent PDE. The slow degeneration of T_α–GDP·P_i rules out the possibility that the turnover of transducin is a major contributor in turning off the cGMP cascade, which occurs within a few seconds under physiological conditions. The phosphorylation of R* by rhodopsin kinase followed by binding to arrestin, which blocks further activation of transducin by R* (Liebman & Pugh, 1980; Wilden et al., 1986a; Sitaramayya & Liebman, 1983), may be the primary events in turning off the cGMP cascade. It is important to emphasize that a total reconstituted system using purified proteins was employed in the current study. The regulation observed in this system may be different under physiological conditions. In other signal-transducing G-proteins, it has been demonstrated that the GTPase activity can be regulated by other protein components. In the case of the ras p21 protein, GTP hydrolysis can be facilitated in the presence of the GAP protein (the GTPase activating protein) [for a review, see McCormick (1989)]. It is not clear whether such factors also exist in the photoreceptor cell to regulate the GTPase activity of transducin. We have tested but failed to detect any effects PDE or the 48-kDa protein may have on the GTPase activity. The turnover time for transducin estimated from the reconstituted system is approximately 30 s. This is consistent with results from previous studies that used more intact sample preparations.

Electromicroscopic studies of intact rod outer segment membranes (Roof et al., 1982) have shown that transducin particles dissociated from the surface of disk membranes after light activation reappeared on the disk membrane after 1 min of incubation in the dark. Furthermore, light-scattering and extra-meta II absorption measurements due to transducin dissociation from the disk membranes in intact rod outer segments suggest that the turnover time of transducin is approximately 1 min (Pepperberg et al., 1988). The suggestion that T_α–GDP·P_i is capable of activating PDE is consistent with the observed effect of AlF_4^- on G-protein activation. It has been proposed that AlF_4^- functions as a phosphate analogue that occupies the γ-phosphate position of the GTP-binding site on G-proteins. Indeed, studies have shown that, in the presence of GDP, AlF_4^- is capable of activating transducin (Bigay et al., 1987). It is likely that the T_α–GDP·AlF_4^- complex is mimicking the structure of T_α-GDP·P_i, and, as a result, T_α–GDP·AlF_4^- activates PDE.

The rate of GTP hydrolysis in retinal rod outer segments has been investigated by microcalorimetry studies (Vuong & Chabre, 1990), which measured the heat generated from the GTP hydrolysis reaction. In a dark-adapted rod outer segment preparation containing GTP, an exothermic reaction was detected approximately 1–4 s after a single light flash. This heat release was assigned to the GTP hydrolysis reaction catalyzed by transducin. On the basis of these results, the authors proposed that since transducin can be deactivated in a few seconds, the hydrolysis of GTP by transducin is fast enough to turn off the cGMP cascade. In order to generate another exothermic reaction from a second flash of light, the sample was required to incubate in the dark for approximately 1 min. This delay was attributed to the time required for the dissociated transducin subunits to reassociate on the disk membrane to participate in another activation cycle. The authors implied that the recycling of the dissociated transducin subunits is the rate-limiting step of the transducin coupling cycle. Although their interpretation of the results from the microcalorimetry measurement is quite different from the conclusion drawn from the present study, the experimental observations of the two studies are in complete agreement. In the pre-steady-state

Scheme II

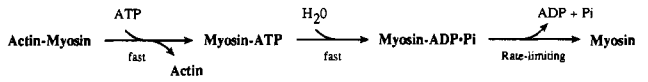

kinetic analyses presented in this paper, the on-site hydrolysis of transducin-bound GTP indeed occurs between 1 and 4 s. This hydrolysis reaction may be the same exothermic reaction detected in the microcalorimetry measurements. However, the slow release of the tightly bound P_i from T_α–GDP·P_i does not involve any heat exchange with the medium and therefore escaped the detection of microcalorimetry. The long-lived T_α–GDP·P_i complex remains active in activating PDE. Thus, the hydrolysis of GTP alone is not sufficient to deactivate transducin, and the deactivation of transducin via GTP hydrolysis and P_i release is not fast enough to account for the rapid shut-off rate of the cGMP cascade. The slow release of P_i from T_α–GDP·P_i may also explain the requirement for a 1-min delay between the detection of exothermic reactions in the microcalorimetry studies.

The basic mechanism of signal transduction utilized by transducin is a subunit dissociation and association cycle regulated via binding to guanine nucleotides. In addition to the signal-transducing G-protein, several well-characterized nucleotide-binding proteins also employ this general nucleotide-mediated switching mechanism. These proteins are involved in cellular functions such as mechanical coupling, as well as in informational transfer during biopolymer synthesis and degradation. Examples of these enzymes include the actin–myosin ATPase in muscle contraction (Hibberd & Trentham, 1986), elongation factor Tu in protein synthesis (Kaziro, 1978), tubulin in microtubule formation (Carlier, 1989), the recA in DNA homologous recombination (Kowalczykowski, 1987), La protease in protein degradation (Menon et al., 1987), kinesin ATPase (Vallee & Shpetner, 1990), and dyneine ATPase (Porter & Johnson, 1989). We have proposed that these enzymes may share a common coupling mechanism and may also have an evolutionary link with the G-protein (Ho et al., 1989). The kinetics of nucleotide (GTP or ATP) hydrolysis of several of these enzymes have been characterized. A careful comparison has revealed that these enzymes utilize a similar mechanism to control the lifetime of the active state of the enzyme for effective coupling action. Similar to transducin, the on-site hydrolysis of the bound nucleotide is fast, which generates a stable enzyme–NDP·P_i complex. This enzyme–NDP·P_i complex remains active in its coupling function before the hydrolytic products are released. The release of the tightly bound P_i or NDP is always the rate-limiting step that controls the deactivation of the enzyme. To illustrate these similarities, the actin–myosin coupling cycle is described briefly below for comparison with the transducin cycle.

Muscle contraction is the result of the sliding motion between actin and myosin filaments. This is accomplished by many cycles of sequential association and dissociation between actin and myosin molecules (Hibberd & Trentham, 1986). In the resting state, myosine heavy chain contains a tightly bound ADP. During the activation process, myosin comes into contact with an actin filament that facilitates the adenine nucleotide exchange of ATP for ADP on the myosin site. The binding of ATP triggers a conformational change in the protein and leads to the dissociation of myosin from the actin filament. After the bound ATP is hydrolyzed and P_i is released, myosin containing ADP can reassociate with another actin subunit along the actin filament for another cycle of activation. As many of these ATP exchange/hydrolysis cycles occur, the actin and myosin filaments slide along each other, resulting in muscle contraction. The equivalence of T_α in this system is myosin, which is the activator and contains the ATP-binding site. Actin, which facilitates the ATP exchange of myosin, is the modulator and is analogous to rhodopsin/$T_{\beta\gamma}$ of the transducin system. The kinetics of the actin–myosin ATP hydrolysis cycle is shown in Scheme II. Similar to transducin, the on-site hydrolysis of bound ATP is fast, but the release of the hydrolytic products, ADP and P_i, is slow and represents the rate-limiting step of the actin–myosin coupling cycle. The myosin–ADP·P_i complex has an active conformation similar to myosin–ATP and is dissociated from actin. The pre-steady-state kinetic analyses of actin–myosin ATPase activity also exhibit an initial burst of P_i formation (Kanazawa & Tonomura, 1965). The dual characteristics of burst kinetics and the existence of stable enzyme–NDP·P_i complexes have also been detected in elongation factor Tu (Kalbitzer et al., 1990), dynein (Holzbaur & Johnson, 1989) and kinesin (Hackney, 1988) ATPases, and tubulin (Melki et al., 1990), as well as other biological coupling enzymes. Furthermore, AlF_4^- has been shown to activate most of these enzymes in the presence of ADP or GDP (Chabre, 1990; Combeau & Carlier, 1988). In view of their similar modes of action, one may suggest that, among the nucleotide-binding proteins, the nucleotide exchange and hydrolysis cycle represents a common motif used by multisubunit enzymes to carry out their cellular coupling functions.

Registry No. PDE, 9068-52-4; GTP, 86-01-1; P_i, 14265-44-2.

References

Applebury, M. L., & Hargrave, P. A. (1986) *Vision Res. 26*, 1881–1895.

Bennett, N., & Dupont, Y. (1985) *J. Biol. Chem. 260*, 4156–4168.

Bigay, J., Deterre, P., Pfister, C., & Chabre, M. (1987) *EMBO J. 6*, 2907–2913.

Bradford, M. M. (1986) *Anal. Biochem. 72*, 248–254.

Carlier, M.-F. (1989) *Int. Rev. Cytol. 115*, 139–170.

Chabre, M. (1990) *Trends Biochem. Sci. 15*, 6–10.

Combeau, C., & Carlier, M.-F. (1988) *J. Biol. Chem. 263*, 17429–17463.

Cornish-Bowden, A. (1976) in *Principles of Enzyme Kinetics*, pp 156–160, Butterworth & Co., England.

Fesenko, E. E., Kolesnikov, S. S., & Lynbarsky, A. L. (1985) *Nature (London) 313*, 310–313.

Frey, S. E., Hingorani, V. N., Su-Tsai, S.-M., & Ho, Y.-K. (1988) *Biochemistry 27*, 8209–8218.

Fung, B. K.-K. (1983) *J. Biol. Chem. 258*, 10495–10502.

Fung, B. K.-K., & Stryer, L. (1980) *Proc. Natl. Acad. Sci. U.S.A. 78*, 2500–2504.

Fung, B. K.-K., Hurley, J. B., & Stryer, L. (1981) *Proc. Natl. Acad. Sci. U.S.A. 78*, 152–156.

Hackney, D. D. (1988) *Proc. Natl. Acad. Sci. U.S.A. 85*, 6314–6318.

Hibberd, M. G., & Trentham, D. R. (1986) *Annu. Rev. Biophys. Biophys. Chem. 15*, 119–161.

Hingorani, V. N., & Ho, Y.-K. (1987) *Biochemistry 26*, 1633–1639.

Ho, Y.-K., & Fung, B. K.-K. (1984) *J. Biol. Chem. 259*, 6694–6699.

Ho, Y.-K., Hingorani, V. N., Navon, S. E., & Fung, B. K.-K. (1989) *Curr. Top. Cell. Regul. 30*, 171–202.

Holzbaur, E. L. F., & Johnson, K. A. (1989) *Biochemistry 28*, 5577–5585.

Hong, K., & Hubbell, W. L. (1973) *Biochemistry 12*, 4517–4527.

Hurley, J. B., & Stryer, L. (1982) *J. Biol. Chem. 257*, 11094–11099.
Kalbitzer, H. R., Feuerstein, J., Goody, R. S., & Wittinghofer, A. (1990) *Eur. J. Biochem. 188*, 355–359.
Kanazawa, T., & Tonomura, Y. (1965) *J. Biochem. Tokyo 57*, 604–615.
Kaziro, Y. (1978) *Biochim. Biophys. Acta 505*, 95–127.
Kowalczykowski, S. C. (1987) *Trends Biochem. Sci. 12*, 141–145.
Kuhn, H., Bennett, N., Michel-Villaz, M., & Chabre, M. (1981) *Proc. Natl. Acad. Sci. U.S.A. 78*, 6873–6877.
Liebman, P. A., & Pugh, E. N., Jr. (1980) *Nature (London) 287*, 734–736.
Liebman, P. A., Park, K. R., & Dratz, E. A. (1987) *Annu. Rev. Physiol. 49*, 765–791.
McCormick, F. (1989) *Cell 56*, 5–8.
Melki, R., Carlier, M.-F., & Pantaloni, D. (1990) *Biochemistry 29*, 8921–8932.
Menon, A. S., Waxman, L., & Goldberg, A. L. (1987) *J. Biol. Chem. 262*, 722–726.
Navon, S. E., & Fung, B. K.-K. (1984) *J. Biol. Chem. 259*, 6686–6693.
Pepperberg, D. R., Kahlert, M., Krause, A., & Hofmann, P. K. (1988) *Proc. Natl. Acad. Sci. U.S.A. 85*, 5531–5535.
Porter, M. E., & Johnson, K. A. (1989) *Annu. Rev. Cell Biol. 5*, 119–151.
Roof, D. J., Korenbrot, J. I., & Heuser, J. E. (1982) *J. Cell Biol. 95*, 501–509.
Sitaramayya, A., & Liebman, P. A. (1983a) *J. Biol. Chem. 258*, 1205–1209.
Sitaramayya, A., & Liebman, P. A. (1983b) *J. Biol. Chem. 258*, 12106–12109.
Stryer, L. (1986) *Annu. Rev. Neurosci. 9*, 87–119.
Vallee, R. B., & Shpetner, H. S. (1990) *Annu. Rev. Biochem. 59*, 909–932.
Vuong, T. M., & Chabre, M. (1990) *Nature (London) 346*, 71–74.
Wilden, U., Hall, S. W., & Kuhn, H. (1986a) *Proc. Natl. Acad. Sci. U.S.A. 83*, 1174–1178.
Wilden, U., Wust, E., Weyland, I., & Kuhn, H. (1986b) *FEBS Lett. 207*, 292–295.
Woodruff, M. L., & Fain, G. L. (1982) *J. Gen. Physiol. 80*, 537–555.
Yee, R., & Liebman, P. A. (1978) *J. Biol. Chem. 253*, 8902–8909.

Structure and Interactions of Ether- and Ester-Linked Phosphatidylethanolamines†

Frederick S. Hing, Prakas R. Maulik, and G. Graham Shipley*
Departments of Biophysics and Biochemistry, Boston University School of Medicine, Boston, Massachusetts 02118
Received March 19, 1991; Revised Manuscript Received June 24, 1991

ABSTRACT: The ether-linked phospholipid 1,2-dihexadecylphosphatidylethanolamine (DHPE) was studied as a function of hydration and in fully hydrated mixed phospholipid systems with its ester-linked analogue 1,2-dipalmitoylphosphatidylethanolamine (DPPE). A combination of differential scanning calorimetry (DSC) and X-ray diffraction was used to examine the phase behavior of these lipids. By DSC, from 0 to 10 wt % H_2O, DHPE displayed a single reversible transition that decreased from 95.2 to 78.8 °C and which was shown by X-ray diffraction data to be a direct bilayer gel to inverted hexagonal conversion, $L_\beta \rightarrow H_{II}$. Above 15% H_2O, two reversible transitions were observed which stabilized at 67.1 and 92.3 °C above 19% H_2O. X-ray diffraction data of fully hydrated DHPE confirmed the lower temperature transition to be a bilayer gel to bilayer liquid-crystalline ($L_\beta \rightarrow L_\alpha$) phase transition and the higher temperature transition to be a bilayer liquid-crystalline to inverted hexagonal ($L_\alpha \rightarrow H_{II}$) phase transition. The lamellar repeat distance of gel-state DHPE increased as a function of hydration to a limiting value of 62.5 Å at 19% H_2O (8.6 mol of water/mol of DHPE), which corresponds to the hydration at which the transition temperatures are seen to stabilize by DSC. Electron density profiles of DHPE, in addition to calculations of the lipid layer thickness, confirmed that DHPE in the gel state forms a noninterdigitated bilayer at all hydrations. Fully hydrated mixed phospholipid systems of DHPE and DPPE exhibited two reversible transitions by DSC. X-ray diffraction data of a mixture containing 10 mol % DPPE identified the lower temperature transition as an $L_\beta \rightarrow L_\alpha$ phase transition and the higher temperature transition as an $L_\alpha \rightarrow H_{II}$ phase transition. Addition of DHPE to DPPE slightly increased the $L_\beta \rightarrow L_\alpha$ transition temperature in a linear fashion, suggesting complete miscibility of the L_β and L_α phases. Increasing amounts of DHPE in DPPE decreased by a greater amount the temperature of the $L_\alpha \rightarrow H_{II}$ transition from the extrapolated value in DPPE. The presence of the ether linkage apparently stabilized the L_β and H_{II} phases and destabilized the L_α phase in the mixed DHPE/DPPE system.

The bilayer matrix of plasma cell membranes is comprised of a complex mixture of different glycerol-based and sphingosine-based polar lipids. The appropriate blend of phospholipids, sphingomyelins, and glycosphingolipids, together with cholesterol, apparently assembles to form the stable lipid bilayer which provides both a general permeability barrier and the matrix into which specific functional membrane proteins (channels, receptors, enzymes, etc.) are asymmetrically incorporated. While many individual membrane lipids [e.g., phosphatidylcholine (PC), sphingomyelin, cerebroside, diglycosyldiglyceride (DGDG)] spontaneously assemble to form

† This work was supported by Research Grant HL-26335 and Training Grants HL-07429 and HL-07291 from the National Institutes of Health.
* Address correspondence to this author at the Department of Biophysics, Boston University School of Medicine.

0006-2960/91/0430-9007$02.50/0